The left panel shows a MODIS granule observed over the Indian Ocean at 0435 UTC on June 22, 2006. The middle and right panels show the retrieved optical thickness and effective particle size, respectively, for the area bounded by the red box indicated in the left panel.

◆IEEE

Uncertainties Associated With the Surface Texture of Ice Particles in Satellite-Based Retrieval of Cirrus Clouds—Part I: Single-Scattering Properties of Ice Crystals With Surface Roughness

Ping Yang, George W. Kattawar, Gang Hong, Patrick Minnis, and Yongxiang Hu

Abstract—Surface roughness of ice crystals is a morphological parameter important to the scattering characteristics of these particles. The intent of this paper, reported in two parts (hereafter, Parts I and II), is to investigate the accuracy associated with some simplifications in calculating the single-scattering properties of roughened ice crystals and to quantify the effect of surface roughness on the retrieval of the optical and microphysical properties of ice clouds from satellite observations. In Part I, two ray-tracing schemes, a rigorous algorithm and an approximate algorithm with a simplified treatment of surface roughness, are employed to calculate the single-scattering properties of randomly oriented hexagonal ice crystals with size parameters in the geometric optics regime. With the rigorous approach, it requires substantial computational effort to accurately account for the multiple external reflections between various roughness facets and the reentries of outgoing rays into the particles in the ray-tracing computation. With the simplified ray-tracing scheme, the ray-tracing calculation for roughened particles is similar to that for smooth particles except that, in the former case, the normal of the particle surface is statistically perturbed for each reflection–refraction event. The simplified ray-tracing scheme can account for most of the effects of surface roughness on particle single-scattering properties without incurring substantial demand on computational resources and, thus, provides an efficient way to compute the single-scattering properties of roughened particles. The effect of ice-crystal surface roughness on the retrieval of the optical thicknesses and effective particle sizes of cirrus clouds is reported in Part II.

Index Terms—Ice crystals, light scattering, ray-tracing, surface roughness.

I. INTRODUCTION

THE RADIATIVE forcing of cirrus clouds is a significant component of the radiation budget in the Earth–atmosphere system. Thus, a better understanding of the radiative characteristics of these clouds is important in improving the current knowledge about the terrestrial climate system and climate feedback [1]–[3]. Satellite observations provide an unprecedented opportunity to quantify the macrophysical and microphysical characteristics of cirrus clouds from a global perspective [4]–[7]. To derive the optical and microphysical properties (particularly, cloud optical thickness and effective particle size) of cirrus clouds from satellite observations, the common retrieval techniques are based on the comparison of measured reflectances with the precomputed lookup libraries of the bidirectional reflection function of cirrus clouds. In practice, a lookup-library-based retrieval method searches for proper entries of cloud optical thickness and effective particle size to minimize the differences between the observed and calculated radiances. In terms of the forward radiative transfer simulations involved in implementing a cirrus retrieval algorithm, the bulk single-scattering properties (i.e., the scattering phase function, single-scattering albedo, and extinction coefficient) of cirrus clouds are indispensable to the development of the aforementioned lookup libraries.

Various balloonborne and aircraft-based observations indicate that ice crystals in cirrus clouds are exclusively nonspherical particles with shapes ranging from small quasi-spherical particles to pristine hexagonal columns/plates and highly irregular habits. The nonsphericity of ice crystals poses significant challenges for obtaining reliable single-scattering properties of these particles. In the past three decades, substantial research efforts from atmospheric research and applied optics communities have been dedicated to the study of the scattering and absorption characteristics of nonspherical ice crystals on the basis of laboratory measurements [8], [9] and various numerical techniques for solving electromagnetic scattering by dielectric particles [10]–[19]. In addition to the overall shape of a scattering particle, the surface texture, i.e., the degree of surface roughness, is also an important morphological parameter that substantially modulates the single-scattering properties of this particle. In the resonant size-parameter region (i.e., the size of a particle is on the order of the incident wavelength), Sun *et al.* [20] investigated the effect of particle surface roughness on the scattering of light by roughened ice columns in the 2-D case, using the well-known finite-difference time-domain technique [21]. Li *et al.* [22] also used the same technique

to study the single-scattering properties of roughened spheres with size parameters in the resonant region. In the geometric optics regime (i.e., the size of a scattering particle is much larger than the incident wavelength), Peltoniemi *et al.* [23] computed the scattering phase function and linear polarization of stochastically deformed spheres. Using the ray-tracing technique, Macke *et al.* [13] and Yang and Liou [18] investigated the surface distortion/roughness effect on the single-scattering properties of roughened ice crystals with large size parameters. According to these previous studies, the overall effect of particle surface roughness (or distortion) on the single-scattering properties of a particle is to smooth out the scattering maxima and peaks in the angular distribution of scattered energy, leading to a featureless phase function. This effect has an important implication in remote sensing of ice clouds from satellite-based radiometric measurements, as demonstrated by Rolland *et al.* [24]. Specifically, Rolland *et al.* [24] showed that the retrieved optical thicknesses and effective sizes based on the phase functions of roughened ice crystals are smaller and larger, respectively, than those derived on the basis of the phase functions of smooth ice crystals. However, in the work of Rolland *et al.* [24], the degree of surface roughness is not quantitatively reported. As the single-scattering properties of scattering particles corresponding to slightly rough, moderately rough, and deeply rough conditions may be quite different, the intent of this paper is to quantify the effect of surface roughness on the retrieval of the optical and microphysical properties of cirrus clouds by quantitatively specifying the degree of particle surface roughness in the precomputed lookup libraries. This paper is reported in two parts (hereafter, Parts I and II). In Part I, we address the rationality and accuracy of the simplifications made in some previous studies (e.g., [13] and [18]) based on the ray-tracing technique for computing the single-scattering properties of roughened ice crystals. In Part II, we quantify the effect of ice-crystal surface roughness on the retrieval of the optical thicknesses and effective particle sizes of cirrus clouds using the bispectral visible/near-infrared method developed by Nakajima and King [25].

II. SCATTERING PHASE FUNCTION OF ICE CRYSTALS WITH SURFACE ROUGHNESS

This paper focuses on the single-scattering properties of roughened ice crystals in the visible and near-infrared spectral region for size parameters in the geometric optics regime. As the physical sizes of ice crystals are normally much larger than visible and near-infrared wavelengths, the geometric optics method is employed in this paper. In the previous studies by Macke *et al.* [13] and Yang and Liou [18] on the basis of the ray-tracing technique, the effect of particle surface roughness is taken into account by assuming that the local normal direction of a roughness facet on the particle surface is randomly tilted from its smooth counterpart for each reflection–refraction event. This approach is an approximation in the sense that the multiple external reflections and refractions involving various roughness facets are neglected. The ray paths in this simplified ray-tracing scheme are also different from those predicted from a rigorous treatment of the particle surface morphological

feature or roughness. To demonstrate the differences between the simplified approach and a rigorous treatment of particle surface roughness in the ray-tracing computation, Fig. 1 shows flowcharts for two ray-tracing schemes for a convex (e.g., a hexagonal column) smooth ice crystal and its roughened counterpart. It should be pointed out that the applicability of the two schemes shown in Fig. 1 is not limited to convex particles, and they are also applicable to complex geometries including concave shapes. In the smooth case [Fig. 1(a)], an externally reflected ray or a transmitted ray (after two refractions) is treated as a scattered ray (or outgoing ray) that is taken into account in the computation of the angular distribution of scattered energy in the ray-tracing calculation. In the case of a roughened particle [Fig. 1(b)], it is necessary to determine whether an externally reflected or transmitted ray emerging from a roughness facet impinges on another roughness facet on the particle surface, i.e., this ray may be reflected by another roughness facet or refracted into the particle. The approach in Macke *et al.* [13] and Yang and Liou [18] to account for the roughness effect uses the ray-tracing scheme shown in Fig. 1(a), except that the normal of a local particle-face on which the ray impinges is randomly perturbed for each reflection–refraction event. Evidently, the approach employed by Macke *et al.* [13] and Yang and Liou [18] is highly simplified in comparison with the rigorous ray-tracing scheme shown in Fig. 1(b) for a roughened particle.

To quantify the accuracy of aforementioned simplification in the work of Macke *et al.* [13] and Yang and Liou [18], we consider the scattering of light by randomly oriented particles with roughened surface in the 2-D case. To define the geometry of a roughened particle, we consider, for example, the line segment between points A and B in Fig. 2. To roughen the particle surface, line AB in Fig. 2 is divided into N segments with an interval of $\Delta t = a/N$, where a is the length of line AB or the semiwidth of the particle. With this division, we define the coordinates of points (x_i, y_i) on the particle surface, where the slopes of piecewise roughened facets abruptly change or discontinue, as follows:

$$(x_1, y_1) = \left(\frac{\sqrt{3}}{2}a, -\frac{1}{2}a \right) \tag{1}$$

$$(x_i, y_i) = \left\lfloor \frac{\sqrt{3}}{2}a + 2\Delta n(1 - 2\xi_{i1}), -\frac{1}{2}a \right.$$
$$\left. + \left(i - \frac{3}{2} + \xi_{i2} \right) \Delta t \right\rfloor,$$
$$i = 2, 3, 4, \ldots, N \tag{2}$$

$$(x_{N+1}, y_{N+1}) = \left(\frac{\sqrt{3}}{2}a, \frac{1}{2}a \right) \tag{3}$$

where ξ_{i1} and ξ_{i2} are random numbers distributed uniformly between zero and one. It is evident from (2) that the parameters Δt and Δn are the mean roughness scales along the directions tangential and normal to the smooth particle surface (i.e., the line segment AB in Fig. 2), respectively. The degree of particle surface roughness increases (or decreases) with the increase of Δn (or Δt). Quantitatively, the degree of surface roughness is proportional to the ratio of Δn to Δt. Specifically, the mean
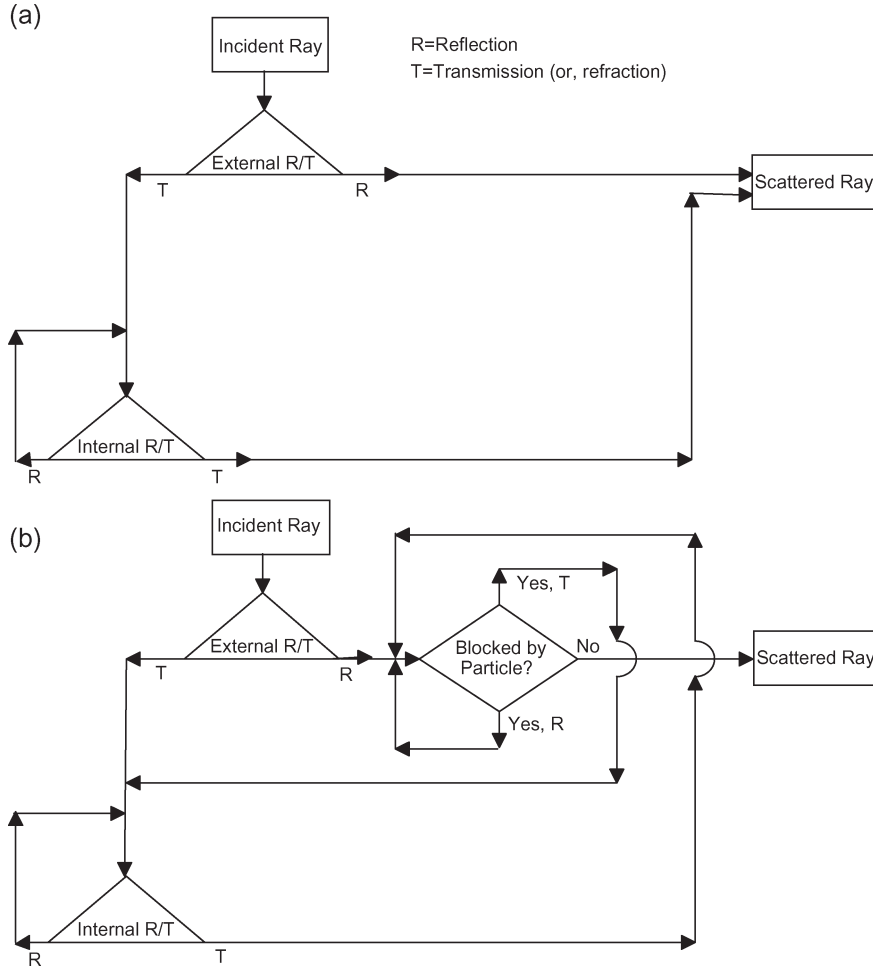
Fig. 1.   Schematic flowcharts for two ray-tracing schemes for convex particles with smooth and roughened surfaces. The scheme illustrated in (a) is a simplified approach. The simplification assumes that the normal of particle surface is randomly disturbed for each reflection–refraction event, but the ray-tracing procedure is the same as that in the case of smooth particles. The scheme illustrated in (b) is a rigorous approach, and the exact particle surface morphology (see Fig. 3) is applied in this scheme.
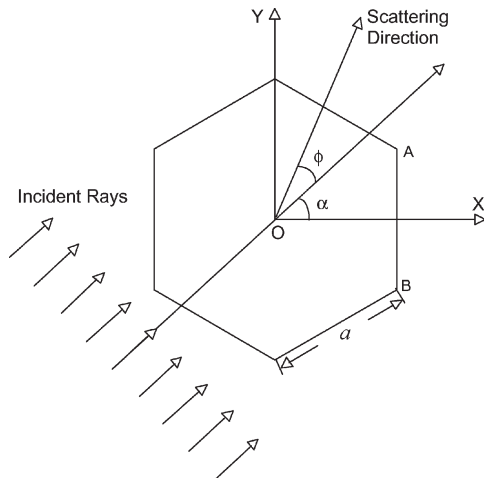

Fig. 2.   Particle orientation and incident scattering configuration in the 2-D case.

slope $\langle s \rangle$ of the roughness facets with respect to the smooth surface is given approximately by

$$\langle s \rangle \approx \Delta n / \Delta t. \tag{4}$$

Fig. 3 shows four surface-roughness configurations specified on the basis of the approach expressed by (1)–(3). The particle size in Fig. 3 is $a = 300$ μm. The upper two panels show two realizations of roughened ice-crystal geometries with $\Delta t = 20$ μm and $\Delta n = 3$ μm, whereas the lower panels are for the case of $\Delta t = 10$ μm and $\Delta n = 6$ μm. Evidently, the particles in the lower panels are rougher than those shown in the upper panels in Fig. 3. For a given degree of surface roughness specified in terms of Δt and Δn, the single-scattering properties of randomly oriented particles with surface roughness need to be averaged over a number of random realizations (or ensembles). In this paper, we use 100 realizations to derive the mean single-scattering properties of roughened ice particles.

As an alternative approach following Yang and Liou [18], we assume that the slopes of the roughened facets on the particle surface can be specified in terms of the Gaussian distribution as follows:

$$f(s) = \frac{1}{\sigma \sqrt{\pi}} \exp(-s^2 / \sigma^2) \tag{5}$$

where f indicates the probability distribution function and $\sigma^2/2$ is the variance of the distribution. For a given reflection and refraction event, we assume that a local facet is randomly tilted
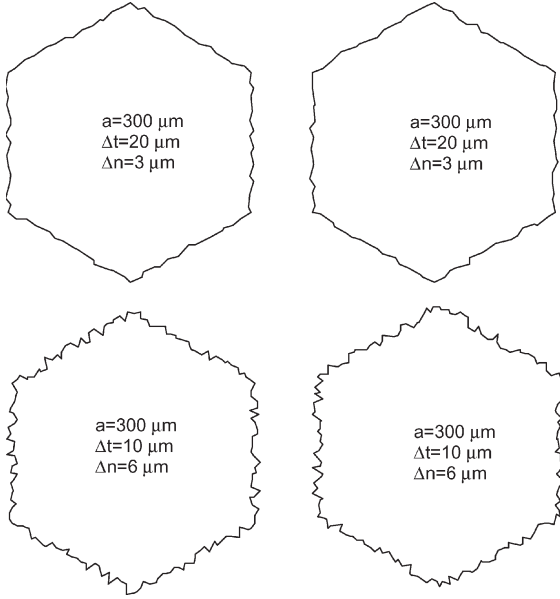
Fig. 3.   Examples of roughened hexagonal particles in the 2-D case. The two parameters Δt and Δn are the mean roughness scales along two directions tangential and normal to the corresponding smooth surface, respectively. The degree of surface roughness for light-scattering calculation is proportional to the ratio of Δn to Δt.

with a slope that is randomly sampled on the basis of (5) and the Box–Muller method [26] as follows:

$$s = \sigma(-\ln \xi_1)^{1/2} \cos(2\pi\xi_2) \qquad (6)$$

where ξ_1 and ξ_2 are random numbers distributed uniformly between zero and one. In this alternative approach, the ray-tracing calculation follows the scheme in Fig. 1(a).

In the 2-D case, the scattered intensity associated with randomly oriented particles can be specified as follows:

$$I_s = \frac{\sigma_s}{r} P(\varphi) I_o \qquad (7)$$

where I_s and I_o are the scattered and incident intensities, respectively, σ_s is the 1-D scattering cross section, r is the distance between the scattering particle and the location where the scattered intensity is observed, and $P(\varphi)$ is the value of the phase function at scattering angle φ. Evidently, the phase function in (7) satisfies the following normalization condition:

$$\int_0^{2\pi} P(\varphi) d\varphi = 1. \qquad (8)$$

For randomly oriented particles, the effect of particle orientations with respect to the incident direction is characterized as follows:

$$P(\varphi) = \frac{\int_0^{2\pi} \sigma_s(\alpha) P(\alpha, \varphi) d\alpha}{\int_0^{2\pi} \sigma_s(\alpha) d\alpha} \qquad (9)$$

where α indicates the orientation of the particle with respect to the incident direction (see Fig. 2). Furthermore, in the frame of the geometric optics method, the scattering phase function can be decomposed as follows:

$$P(\varphi) = \frac{1}{2\omega} P_d(\varphi) + f_\delta \delta(\varphi) + \left(1 - f_\delta - \frac{1}{2\omega}\right) P_{\text{ray}}(\varphi) \qquad (10)$$

where P_d and P_{ray} are the phase function components from the contributions of diffraction and reflected/refracted rays, respectively, $\delta(\varphi)$ is the Dirac–delta function, and f_δ is the fraction of the delta transmission associated with the ray transmission through two parallel faces [11], [14]. Note that $P_d(\varphi)$ and $P_{\text{ray}}(\varphi)$ satisfy the normalization condition in (8). In this paper, we concentrate on the effect of particle surface roughness on $P_{\text{ray}}(\varphi)$, because $P_d(\varphi)$ peaks in the forward direction and can be analytically derived.

III. RESULTS AND DISCUSSIONS

Fig. 4 shows the effect of surface roughness on the scattering properties of 2-D randomly oriented ice crystals at a wavelength of 0.66 μm. The refractive index of ice [27] at this wavelength is $(m_r, m_i) = (1.3078, 1.66 \times 10^{-8})$. The upper panel in Fig. 4 shows P_{ray} defined in (10) for vertically and horizontally polarized radiation in the case of a smooth particle surface. Evidently, a strong scattering peak is observed at $22°$ scattering angle, which corresponds to the well-known $22°$ halo. The sensitivity of the phase function to the polarization configuration is noticed in side scattering directions from $80°$ to $155°$. The detailed scattering features of randomly oriented 2-D smooth hexagons are not discussed here, because they have been reported in the literature [10], [28].

The lower panel in Fig. 4 shows the phase functions of roughened particles for two polarization configurations. Evidently, surface roughness smoothes out the scattering peaks observed in the case of smooth surface. Additionally, the effect of surface roughness also reduces the sensitivity of the phase function to the polarization configuration of the incident radiation, as is obvious from a comparison of the results in the upper and lower panels in Fig. 4. Furthermore, the value of $P_{\text{ray}}(\varphi)$ in the forward directions ($\varphi < 10°$) is much larger in the case of roughened particles than in the case of smooth particles. This is because the energy associated with delta transmission spreads into a small angular interval around the forward direction due to the effect of the particle surface roughness, as is evident from the fact that the delta transmission fractions in the smooth case are 0.1702 and 0.1716 for vertical and horizontal polarization configurations, respectively, and are 8.867×10^{-4} and 9.096×10^{-4} in the case of roughened particles.

The physical sizes of the particles involved in Fig. 4 are much larger than the incident wavelength. Thus, the scattered energy due to the contribution of diffraction is concentrated in the forward direction. As an accurate approximation, it can be assumed that the asymmetry factor associated with $P_d(\varphi)$ in (10) is approximately one. Thus, from (10), the total asymmetry factor for the phase function of the scattering particles can be approximated as follows:

$$g \approx \frac{1}{2\omega} + f_\delta + \left(1 - f_\delta - \frac{1}{2\omega}\right) g_{\text{ray}}, \qquad (11)$$
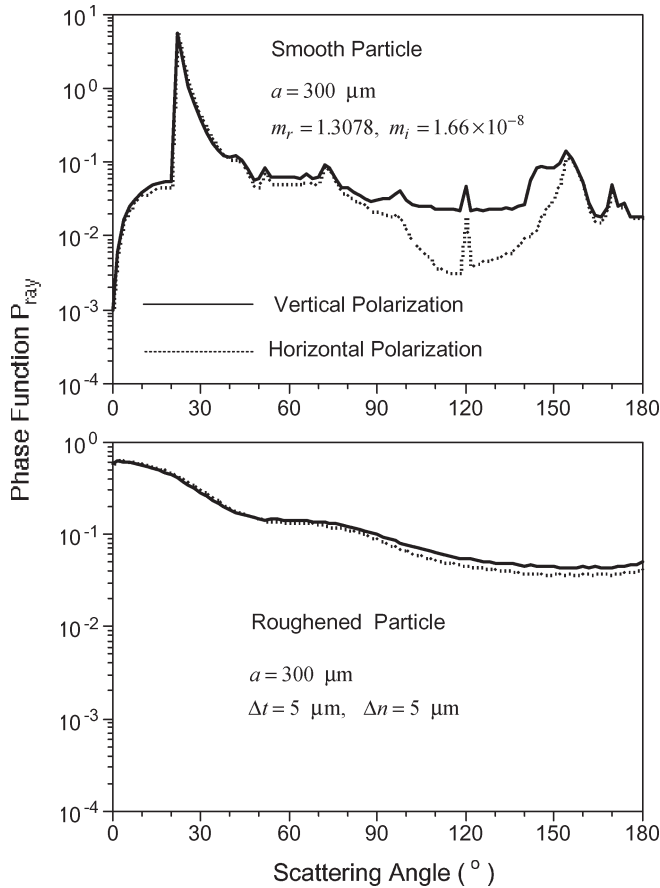
Fig. 4.   Phase functions associated with the scattering of polarized light by 2-D hexagonal particles with smooth and rough surfaces at a wavelength of 0.66 μm. The particles are randomly oriented.

where g_{ray} is associated with the normalized $P_{\mathrm{ray}}(\varphi)$. The roughness effect reduces the total asymmetry factor. For example, the g factors for the phase functions for the vertical and horizontal polarization configurations are 0.8873 and 0.9202, respectively, in the case of smooth particles, whereas the counterparts for the roughened particles are 0.7806 and 0.80179, respectively.

Fig. 5 shows the phase functions associated with the scattering of polarized light by 2-D hexagonal ice particles at a near-infrared wavelength of 2.13 μm. At this wavelength, the refractive index is $1.267 + i5.5682 \times 10^{-4}$, and the particles have a considerable amount of absorption. The overall features shown in Fig. 5 are similar to those shown in Fig. 4. Again, it is evident that the primary effect of surface roughness is to smooth the phase functions. The g factors for the phase functions for the vertical and horizontal polarization configurations are 0.9168 and 0.94137, respectively, in the case of smooth particles, whereas the counterparts for the roughened particles are 0.8860 and 0.9076, respectively.

Fig. 6 shows the variation of the asymmetry factor versus Δt in the cases of $\Delta n = 1$ μm and $\Delta n = 5$ μm at wavelengths 0.66 μm and 2.13 μm. As evident from (4), the degree of surface roughness decreases with increasing Δt for a fixed Δn. Thus, Fig. 6 shows that the asymmetry factor monotonically decreases with the increase of the degree of surface roughness. Note that, in the case of smooth surface, the asymmetry factors
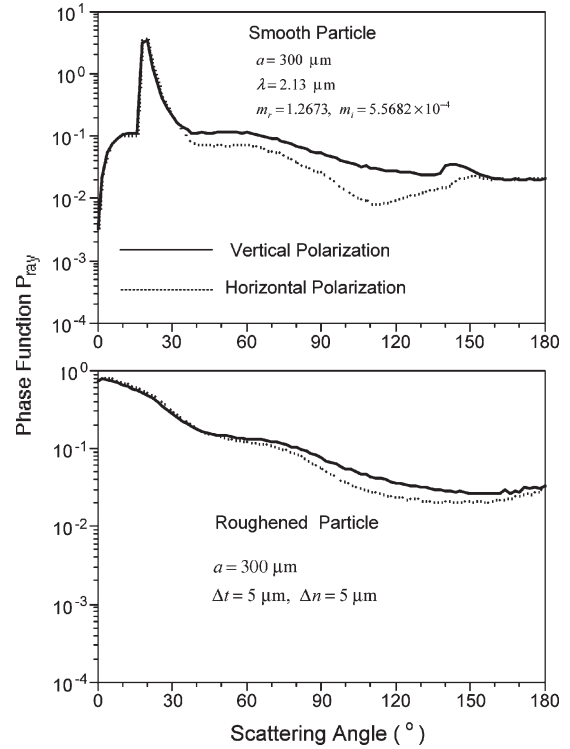

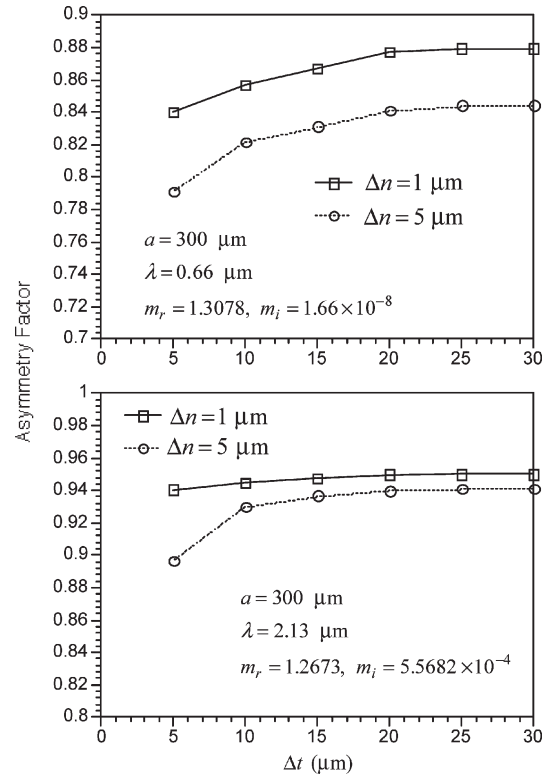Fig. 5.   Same as Fig. 4, except for wavelength 2.13 μm.

Fig. 6.   Variation of the asymmetry factor versus roughness parameter Δt in cases of $\Delta n = 1$ μm and $\Delta n = 5$ μm. Note that the degree of surface roughness is proportional to the ratio of Δn to Δt.

corresponding to the results in the upper and lower panels of Fig. 6 are 0.9040 and 0.9564, respectively.

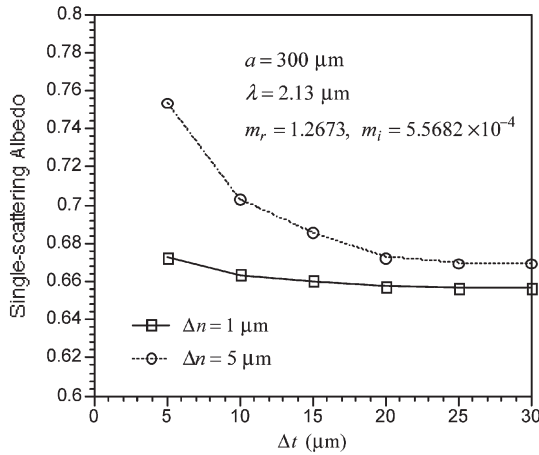Fig. 7 shows the effect of surface roughness on the single-scattering albedo at wavelength 2.13 μm. Note that the

Fig. 7.   Variation of the single-scattering albedo versus roughness parameter Δt in cases of $\Delta n = 1$ μm and $\Delta n = 5$ μm. Note that the degree of surface roughness is proportional to the ratio of Δn to Δt.

single-scattering albedo of ice crystals at wavelength 0.66 μm is essentially one regardless of the roughness condition, as the imaginary part of the refractive index of ice at this wavelength is extremely small. It is evident from Fig. 7 that, with increasing Δt for a given Δn, the single-scattering albedo decreases, i.e., surface roughness increases the single-scattering albedo. The corresponding single-scattering albedo in the case of smooth surface is 0.6468. In the geometric optics regime, the absorption of a scattering particle is proportional to the mean path length of rays within the particle. Thus, the results in Fig. 7 indicate that surface roughness decreases the mean path length for the rays within ice crystals.

To compare the rigorous ray-tracing scheme [Fig. 1(b)] for roughened particles and the simplified version employed by Macke *et al.* [13] and Yang and Liou [18], Fig. 8 shows the phase functions for two roughness conditions for unpolarized incident radiation. For the phase functions in the upper panel of Fig. 8, the asymmetry factors computed from the rigorous ray-tracing scheme and the simplified version are 0.8399 and 0.84028, respectively, whereas the results are 0.8141 and 0.81366 for the phase functions in the lower panel of Fig. 8.

Fig. 9 is the same as Fig. 8, except that Fig. 9 is for a near-infrared wavelength of 2.13 μm. At this wavelength, the phase functions calculated from the rigorous and approximate ray-tracing schemes are similar, particularly, in the case of a moderate roughness condition (the upper panel). When the surfaces of ice crystals are very rough (the lower panel), the phase functions computed from the two schemes show noticeable differences for scattering angles larger than 150°. For the results shown in the upper panel, the asymmetry factors calculated from the rigorous and approximate schemes are 0.9405 and 0.9485, respectively, i.e., the relative difference of the two results, $(g_{approximate} - g_{rigorous})/g_{rigorous}$, is 0.81%. In the case of a deep roughness condition (the lower panel in Fig. 9), the asymmetry factors calculated from the rigorous and approximate schemes are 0.9246 and 0.9301, respectively, i.e., the relative difference of the two results, $(g_{approximate} - g_{rigorous})/g_{rigorous}$, is 0.59%. In terms of the single-scattering albedo (ω), the differences between the two solutions are $(\omega_{approximate} - \omega_{rigorous})/\omega_{rigorous} = -2.2\%$ and 3.3% for
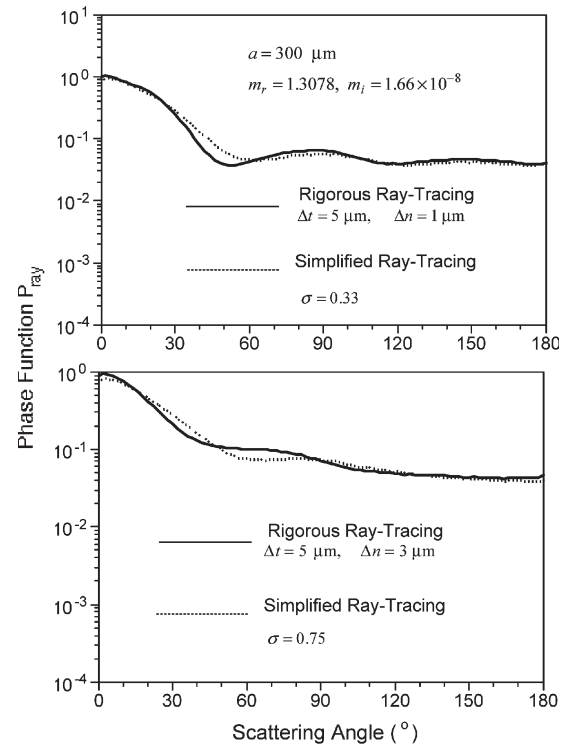
Fig. 8.   Comparison of the phase functions computed from two ray-tracing schemes.

Fig. 9.   Same as Fig. 8, except for wavelength 2.13 μm.

the results shown in the upper and lower panels in Fig. 9, respectively.

For the phase functions in Figs. 8 and 9, the results computed from the rigorous ray-tracing scheme are similar to those based on the simplified ray-tracing scheme. However, in the case of $\lambda = 0.66$ μm, some differences between the two solutions

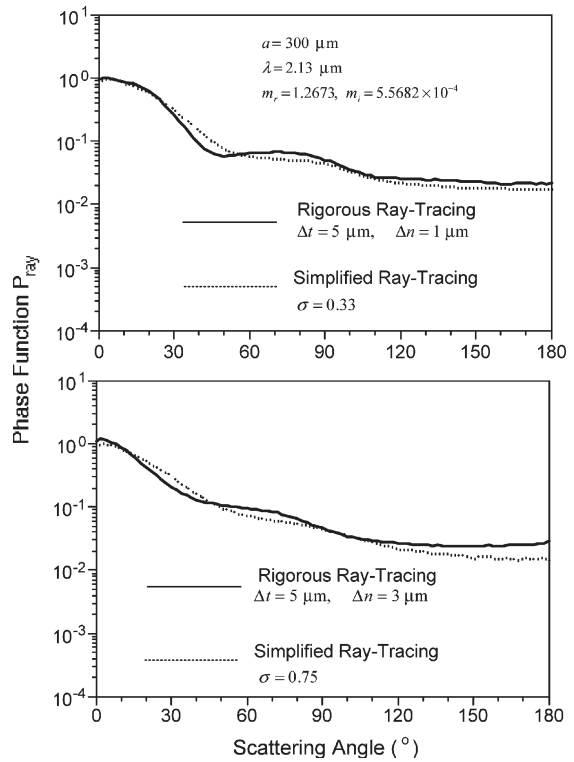are noticed at scattering angles between $20°$ and $80°$. These differences are due to two mechanisms. First, the ray paths in the two ray-tracing schemes are different, as the simplified ray-tracing scheme neglects the external reflections between roughness facets and the reentry of refracted rays into the scattering particles. Second, the surface roughness is specified differently in these two ray-tracing schemes. In the rigorous ray-tracing scheme, the surface roughness is specified by two morphological parameters Δt and Δn. In the simplified ray-tracing scheme, particle surface roughness is specified by one parameter σ on the basis of the Gaussian distribution for the slopes of roughness facets assumed for the perturbation of the normal of the particle surface for each reflection and refraction event. The comparison of the phase functions computed from the rigorous and simplified schemes at wavelength 2.13 μm is similar to the case of visible light. However, the solutions derived from the two ray-tracing schemes show noticeable differences for scattering angles larger than $130°$ in the case of deep roughness. The differences may be caused by different ray paths in the rigorous and simplified ray-tracing schemes.

It is evident from Figs. 8 and 9 that, regardless of some moderate differences between the phase functions computed from the two ray-tracing schemes, the simplified ray-tracing scheme produces the major effect of surface roughness on the single-scattering properties. In terms of computer CPU time, the demand on computational resources by the rigorous ray-tracing method is several orders of magnitude larger than that of the simplified ray-tracing scheme. The difference between the computational requirements associated with the two ray-tracing schemes is more significant in the 3-D case. Computationally, the rigorous ray-tracing scheme is impractical in the 3-D case.

IV. Summary

We investigated two ray-tracing schemes for calculating the single-scattering properties of randomly oriented particles with size parameters in the geometric optics regime. For a rigorous treatment of surface roughness in ray-tracing calculations, the particle surface morphology is defined in terms of two parameters that specify the roughness scales along tangential and normal directions. In this rigorous ray-tracing scheme, the multiple external reflections between various roughness facets and the reentries of outgoing rays into the particles are taken into account. This approach requires significant computational effort in practice. In the simplified ray-tracing scheme, the ray-tracing calculation is carried out in the same way as in the case of smooth particles, except that the normal of the particle surface is perturbed for each reflection–refraction event. The present results show that the simplified ray-tracing scheme can approximately account for the effect of surface roughness on particle single-scattering properties. Thus, the simplified ray-tracing scheme provides an efficient way to compute the single-scattering properties of roughened particles with size parameters in the geometric optics regime. Furthermore, it should be pointed out that the rigorous treatment of surface roughness in ray-tracing calculation is quite challenging in the case of 3-D particles with complicated geometries. However,

it is straightforward to generalize the simplified ray-tracing scheme to 3-D roughened particles with various shapes.

For the 2-D scattering problem investigated in this paper, the effect of surface roughness is to smooth the phase functions at both visible and near-infrared wavelengths and increase the values of the single-scattering albedo at near-infrared wavelengths. This feature has an important implication to the forward radiative transfer simulation involved in the bispectral method developed by Nakajima and King [25] for retrieving cloud properties (this issue will be addressed in detail in Part II).

To be consistent with previous studies by Macke *et al.* [13] and Yang and Liou [18], this paper showed that surface roughness alternates the asymmetry factor of the phase function in the 2-D case. Specifically, the asymmetry factors for 2-D roughened particles are smaller than their counterparts for 2-D smooth particles. Stephens *et al.* [3] demonstrated that the impact of ice clouds on climate is sensitive to the asymmetry factor of the bulk phase function of ice crystals. Thus, the effect of surface roughness on the parameterization of the asymmetry factor for application to the radiative transfer schemes involved in climate models deserves investigation, although this topic is beyond the scope of this paper.

References

[1] K.-N. Liou, "Influence of cirrus clouds on weather and climate processes: A global perspective," *Mon. Weather Rev.*, vol. 114, no. 6, pp. 1167–1199, Jun. 1986.

[2] D. K. Lynch, K. Sassen, D. O'C. Starr and G. Stephens, Eds., *Cirrus*, New York: Oxford Univ. Press, 2002.

[3] G. L. Stephens, S. C. Tsay, P. W. Stackhouse, and P. J. Flatau, "The relevance of the microphysical and radiative properties of cirrus clouds to climate and climatic feedback," *J. Atmos. Sci.*, vol. 47, no. 14, pp. 1742–1753, Jul. 1990.

[4] P. Minnis, Y. Takano, and K.-N. Liou, "Inference of cirrus cloud properties using satellite-observed visible and infrared radiances. Part I: Parameterization of radiance fields," *J. Atmos. Sci.*, vol. 50, no. 9, pp. 1279–1304, May 1993.

[5] P. Minnis, P. W. Heck, and D. F. Young, "Inference of cirrus cloud properties using satellite-observed visible and infrared radiances. Part II: Verification of theoretical cirrus radiative properties," *J. Atmos. Sci.*, vol. 50, no. 9, pp. 1305–1322, May 1993.

[6] M. D. King, Y. J. Kaufman, W. P. Menzel, and D. Tanre, "Remote sensing of cloud, aerosol, and water vapor properties from the Moderate Resolution Imaging Spectrometer (MODIS)," *IEEE Trans. Geosci. Remote Sens.*, vol. 30, no. 2, pp. 2–27, Jan. 1992.

[7] S. Platnick, M. D. King, S. A. Ackerman, W. P. Menzel, B. A. Baum, J. C. Riedi, and R. A. Frey, "The MODIS cloud products: Algorithms and examples from Terra," *IEEE Trans. Geosci. Remote Sens.*, vol. 41, no. 2, pp. 459–473, Feb. 2003.

[8] K. Sassen and K. N. Liou, "Scattering of polarized laser light by water droplet, mixed-phase and ice crystal clouds. Part I: Angular scattering patterns," *J. Atmos. Sci.*, vol. 36, no. 5, pp. 838–851, May 1979.

[9] B. Barkey, M. Bailey, K. N. Liou, and J. Hallet, "Light-scattering properties of plate and column ice crystals generated in a laboratory cold chamber," *Appl. Opt.*, vol. 41, no. 27, pp. 5792–5796, Sep. 2002.

[10] Q. Cai and K.-N. Liou, "Polarized light scattering by hexagonal ice crystals: Theory," *Appl. Opt.*, vol. 21, no. 19, pp. 3569–3580, Oct. 1982.

[11] Y. Takano and K.-N. Liou, "Solar radiative transfer in cirrus clouds. Part I: Single-scattering and optical properties of hexagonal ice crystals," *J. Atmos. Sci.*, vol. 46, no. 1, pp. 3–19, Jan. 1989.

[12] A. Macke, "Scattering of light by polyhedral ice crystals," *Appl. Opt.*, vol. 32, no. 15, pp. 2780–2788, May 1993.

[13] A. Macke, J. Mueller, and E. Raschke, "Single scattering properties of atmospheric ice crystals," *J. Atmos. Sci.*, vol. 53, no. 19, pp. 2813–2825, Oct. 1996.

[14] M. I. Mishchenko and A. Macke, "Incorporation of physical optics effects and δ-function transmission," *J. Geophys. Res.*, vol. 103, no. D2, pp. 1799–1805, 1998.

[15] M. I. Mishchenko and A. Macke, "How big should hexagonal ice crystals be to produce halos?" *Appl. Opt.*, vol. 38, no. 9, pp. 1626–1629, Mar. 1999.

[16] K. Muinonen, "Scattering of light by crystals: A modified Kirchhoff approximation," *Appl. Opt.*, vol. 28, no. 15, pp. 3044–3050, Aug. 1989.

[17] P. Yang and K. N. Liou, "Geometric-optics-integral-equation method for light scattering by nonspherical ice crystals," *Appl. Opt.*, vol. 35, no. 33, pp. 6568–6584, Nov. 1996.

[18] P. Yang and K. N. Liou, "Single-scattering properties of complex ice crystals in terrestrial atmosphere," *Contrib. Atmos. Phys.*, vol. 71, no. 2, pp. 223–248, 1998.

[19] A. J. Baran, P. Yang, and S. Havemann, "Calculation of the single-scattering properties of randomly oriented hexagonal ice columns: A comparison of the T-matrix and the finite-difference time-domain methods," *Appl. Opt.*, vol. 40, no. 24, pp. 4376–4386, Aug. 2001.

[20] W. B. Sun, N. Loeb, G. Videen, and Q. Fu, "Examination of surface roughness on light scattering by long ice columns by use of a two-dimensional finite-difference time-domain algorithm," *Appl. Opt.*, vol. 43, no. 9, pp. 1957–1964, Mar. 2004.

[21] S. K. Yee, "Numerical solution of initial boundary value problems involving Maxwell's equations in isotropic media," *IEEE Trans. Antennas Propag.*, vol. AP-14, no. 3, pp. 302–307, May 1966.

[22] C. Li, G. W. Kattawar, and P. Yang, "Effects of surface roughness on light scattering by small particles," *J. Quant. Spectrosc. Radiat. Transf.*, vol. 89, no. 1–4, pp. 123–131, Nov./Dec. 2004.

[23] J. I. Peltoniemi, K. Lumme, K. Muinonen, and W. M. Irvine, "Scattering of light by stochastically rough particles," *Appl. Opt.*, vol. 28, no. 19, pp. 4088–4095, Oct. 1989.

[24] P. Rolland, K.-N. Liou, M. D. King, S. C. Tsay, and G. M. McFarquhar, "Remote sensing of optical and microphysical properties of cirrus clouds using MODIS channels: Methodology and sensitivity to assumptions," *J. Geophys. Res.*, vol. 105, no. D9, pp. 11 721–11 738, 2000.

[25] T. Nakajima and M. D. King, "Determination of the optical thickness and effective particle radius of clouds from reflected solar radiation measurements. Part I: Theory," *J. Atmos. Sci.*, vol. 47, no. 15, pp. 1878–1893, Aug. 1990.

[26] W. H. Press, S. A. Teukolsky, W. T. Vetterling, and B. P. Flannery, *Numerical Recipes in C*, 2nd ed. New York: Cambridge Univ. Press, 1992, p. 289.

[27] S. G. Warren, "Optical constants of ice from the ultraviolet to the microwave," *Appl. Opt.*, vol. 23, no. 8, pp. 1206–1225, Apr. 1984.

[28] P. Yang and K. N. Liou, "Light scattering by hexagonal ice crystals: Solution by a ray-by-ray integration algorithm," *J. Opt. Soc. Amer. A, Opt. Image Sci.*, vol. 14, no. 9, pp. 2278–2288, Sep. 1997.

Ping Yang received the B.S. degree in theoretical physics from Lanzhou University, Lanzhou, China, in 1985, the M.S. degree in atmospheric physics from the Lanzhou Institute of Plateau Atmospheric Physics, Chinese Academy of Sciences, Lanzhou, in 1988, and the Ph.D. degree in meteorology from the University of Utah, Salt Lake City, in 1995.

After graduation, he remained for two years with the University of Utah, where he was a Research Associate. He was an Assistant Research Scientist with the University of California at Los Angeles, Los Angeles, and an Associate Research Scientist with the Goddard Earth Sciences and Technologies Center, University of Maryland Baltimore County, Baltimore. He is currently an Associate Professor with the Department of Atmospheric Sciences, Texas A&M University, College Station. He is a member of the Moderate Resolution Imaging Spectroradiometer Science Team. His research interests are in the areas of remote sensing and radiative transfer. He has been actively conducting research in the modeling of the optical and radiative properties of clouds and aerosols, in particular, cirrus clouds, and their applications to spaceborne and ground-based remote sensing. He has coauthored more than 100 peer-reviewed publications. He is currently an Associate Editor for the *Journal of Atmospheric Sciences*, the *Journal of Quantitative Spectroscopy and Radiative Transfer*, and the *Journal of Applied Meteorology and Climatology*.

Prof. Yang was the recipient of a Best Paper Award from the Climate and Radiation Branch, NASA Goddard Space Center in 2000, the U.S. National Science Foundation CAREER Award in 2003, and the Dean's Distinguished Achievement Award for Faculty Research, College of Geosciences, Texas A&M University in 2004.

George W. Kattawar received the M.S. and Ph.D. degrees from Texas A&M University, College Station.

He is currently a Professor of physics with the Department of Physics, Texas A&M University. He is the author/coauthor of over 120 publications in fields ranging from radiative transfer in atmosphere–ocean systems to quantum optics. His present research interests include radiative transfer in realistic planetary atmospheres and oceans with inclusion of polarization and high-resolution spectroscopic calculations such as Raman and Rayleigh–Brillouin scattering, Mueller matrix imaging in turbid media, and electromagnetic scattering from irregularly shaped objects.
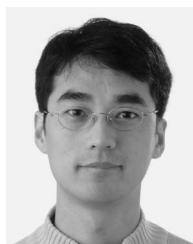
Gang Hong received the B.S. degree in atmospheric sciences from the Nanjing Institute of Meteorology, Nanjing, China, in 1995 and the Ph.D. degree in environmental physics and remote sensing from the University of Bremen, Bremen, Germany, in 2004.

He is currently an Assistant Research Scientist with the Department of Atmospheric Sciences, Texas A&M University, College Station. His recent research focuses on retrieving ice-cloud and aerosol properties and investigating radiative properties of clouds from the moderate resolution imaging spectrometer and atmospheric infrared sounder measurements. He is also working on the simulation of the optical properties of nonspherical ice crystals at millimeter and submillimeter wavelengths.

Patrick Minnis received the B.E. degree in materials science and metallurgical engineering from Vanderbilt University, Nashville, TN, in 1972, the M.S. degree in atmospheric science from Colorado State University, Fort Collins, in 1978, and the Ph.D. degree in meteorology from the University of Utah, Salt Lake City, in 1991.

He is currently a Senior Research Scientist with the Climate Sciences Branch, NASA Langley Research Center, Hampton, VA, where he has served for more than 25 years. His research is focused on the remote sensing of clouds and surface properties from satellite imagery for weather and climate investigations. He is the author/coauthor of over 150 peer-reviewed publications. He is a member of the Clouds and the Earth's Radiant Energy System, Atmospheric Radiation Measurement, and ICES at Science Teams and leads a research group conducting analyses of polar-orbiting and geostationary satellite data for field missions, operational aircraft icing condition diagnosis, and contrail research. He is currently an Editor for the *Journal of Atmospheric Sciences*.

Dr. Minnis was the recipient of the NASA medals for Exceptional Scientific Achievement in 1993 and Exceptional Achievement in 2005 and the AMS Henry G. Houghton Award for Atmospheric Physics in 1998.

Yongxiang Hu received the Ph.D. degree in atmospheric sciences from the University of Alaska, Fairbanks, in 1994.

He was a Postdoctoral Researcher with the College of William and Mary, Williamsburg, VA, and was a Research Professor with Hampton University, Hampton, VA. Since 1999, he has been with NASA Langley Research Center, Hampton, VA, where he is currently a Senior Research Scientist with the Climate Sciences Branch. His research interests include radiative transfer, passive and active atmospheric remote sensing, and satellite onboard data analysis.